

# SpecNet: Spectral Domain Convolutional Neural Network

Bochen Guan\*, Jinnian Zhang\*, William A. Sethares, Richard Kijowski and Fang Liu  
University of Wisconsin-Madison

## Abstract

*The memory consumption of most Convolutional Neural Network (CNN) architectures grows rapidly with increasing depth of the network, which is a major constraint for efficient network training and inference on modern GPUs with limited memory. Several studies show that the feature maps (as generated after the convolutional layers) are the main bottleneck in this memory problem. Often, these feature maps mimic natural photographs in the sense that their energy is concentrated in the spectral domain. Although embedding CNN architectures in the spectral domain is widely exploited to accelerate the training process, we demonstrate that it is also possible to use the spectral domain to reduce the memory footprint by proposing a Spectral Domain Convolutional Neural Network (SpecNet) that performs both the convolution and the activation operations in the spectral domain. SpecNet exploits a configurable threshold to force small values in the feature maps to zero, allowing the feature maps to be stored sparsely. SpecNet also employs a special activation function that preserves the sparsity of the feature maps while effectively encouraging the convergence of the network. The performance of SpecNet is evaluated on three competitive object recognition benchmark tasks (MNIST, CIFAR-10, and SVHN), and compared with four state-of-the-art implementations (LeNet, AlexNet, VGG, and DenseNet). Overall, SpecNet is able to reduce memory consumption by about 60% without significant loss of performance for all tested network architectures.*

## 1. Introduction

Deep convolutional neural networks have made significant progress on various tasks in recent years [20, 13, 12, 25, 27]. Current successful deep CNNs such as ResNet [12] and DenseNet [13] typically include over 100 layers and require large amounts of training data. Training these models becomes computationally and memory intensive, especially when limited resources are available [5]. Therefore, it is essential to reduce the memory requirements to allow better network training and deployment, such as applying deep

CNNs to embedded systems and cell phones.

Several studies [14, 38] show that the intermediate layer outputs (feature maps) are the primary contributors to this memory bottleneck. Existing methods such as model compression [40, 6, 11, 8] and scheduling [31, 4, 41], do not directly address the storage of feature maps. By transforming the convolutions into the spectral domain, we target the memory requirements of feature maps.

In contrast to [14], which proposes an efficient encoded representation of feature maps in the spatial domain, we exploit the property that the energy of feature maps is concentrated in the spectral domain [14]. Values that are less than a configurable threshold are forced to zero, so that the feature maps can be stored sparsely. We call this approach the Spectral Domain Convolutional Neural Network (SpecNet). In this new architecture, convolutional and activation layers are implemented in the spectral domain. The outputs of convolutional layers are equal to the multiplication of non-zero entries of the inputs and kernels. The activation function is designed to preserve the sparsity and symmetry properties of the feature maps in the spectral domain, and also allow effective derivative computation in back propagation. It is notable that the sparsity of kernels in their spectral representations [34, 2] will use more memory. In contrast, our work is focused on designing a network to optimize the feature maps and kernels in SpecNet are stored in spatial domain.

More specifically, this paper contributes the following:

- A new CNN architecture (SpecNet) that performs convolution and activation in the spectral domain. Feature maps are thresholded and compressed to allow reducing model memory by only computing and saving non-zero entries. Kernels will not be stored in spectral domain and avoid the extra memory consumption.
- A spectral domain activation function is applied to both the real and imaginary parts of the input feature maps, preserving the sparsity property and ensuring effective network convergence during training.
- Extensive experiments are conducted to show the effectiveness of SpecNet using different architectures at multiple computer vision tasks. For example, a

\*Equal contribution

SpecNet implementation of DenseNet architecture can reach up to 60% reduction of the memory usage on the SHVN dataset without significant loss of accuracy (95.8% testing accuracy compared with 98.2% accuracy of the original implementation).

## 2. Related Work

### 2.1. Model Compression

Model compression can be achieved in several ways including quantization, pruning and weight decomposition.

With quantization, the values of filter kernels in the convolutional layers and weight matrices in fully-connected layers are quantized into a limited number of levels. This can decrease the computational complexity and reduce memory cost [40, 10]. The extreme case of quantization is binarization [6, 1] which uses only  $\pm 1$  to represent all values of the weights, resulting in dramatic memory reduction but risking potentially degraded performance.

Pruning and weight decomposition are other approaches to model compression. The key idea in pruning is to remove unimportant connections. Some initial work [11] focused on using weight decay to sparsify the connections in neural networks while more recent work [39, 24] applied structured sparsity regularizers to the weights. Instead of selecting redundant connections, [3] proposed a compression technique that fixed a random connectivity pattern and required the CNN to train around it. Weight decomposition is based on a low-rank decomposition of the weights in the network. The SVD is an efficient method for decomposition, and has proven to be successful in shrinking the size of the model [8]. Other work [26, 42] uses PCA for rank selection. The pruning and weight decomposition attempt to reduce the size of the model so that it is more easily deployed in embedded systems or smart phones. Overall, the aforementioned methods are focused on compressing weights to reduce the model size, and further reduce the size of feature maps. In contrast, SpecNet directly reduces the memory consumption by sparsifying the feature maps and storing them efficiently. The two methods may be combined to save memory.

### 2.2. Memory Sharing

Since the 'life-time' of feature maps (the amount of time data from a given layers must be stored) is different in each layer, it is possible to design data reuse methods to reduce memory consumption. [31] observes the feature maps in some layers that are responsible for most of the memory consumption are relatively cheap to compute. By storing the output of the concatenation, batch normalization and ReLU layers in shared memory, DenseNet can achieve more than  $4x$  memory saving, compared to the original implementation that allocates new memory for these layers. A

more general algorithm for designing memory sharing patterns can be found in [4]. It can be applied to CNNs and RNNs with sublinear memory cost compared to the original implementations. Recently, an approach called Smart-Pool [41] has been proposed to provide an even more fine-grained memory sharing and reduction strategy.

### 2.3. Representation of Feature Maps in the Spatial Domain

The above methods are not focused on compressing feature maps directly. [14] employed two classes of layer-specific encoding schemes to encode and store the feature maps in the time domain, and to decode the data for back propagation. The additional encoding and decoding process increase the computational complexity. In SpecNet, the architecture is designed for sparse storage of feature maps in the spectral domain, which is more computationally efficient.

[38] proposed a method to extract intrinsic representations of the feature maps while preserving the discriminability of the features. It can achieve a high compression ratio, but the training process involves a pre-trained CNN and solving an optimization problem. SpecNet does not require additional modules in the training process and is easier to implement.

### 2.4. CNN in the Spectral Domain

Some pilot studies have attempted to combine Fast Fourier Transform (FFT) and Wavelet transforms with CNNs [34, 32, 28, 9]. However, most of these works aim to make the training process faster by replacing the traditional convolution operation with the FFT and dot product of the inputs and kernel in spectral domain [32, 28]. Wavelet CNN [9] concatenates the feature maps and multi-resolution features captured by the wavelet transform of the input images to improve the classification accuracy. These methods do not attempt to reduce memory, and several works (such as the Wavelet CNN) require more memory in order to achieve optimal performance. In contrast, SpecNet uses the FFT to reduce memory consumption and its computation complexity depends on certain input parameters, which is quite different from most FFT-based CNN implementations.

## 3. SpecNet

The key idea of SpecNet rests on the observation that feature maps, like most natural images, tend to have compact energy in the spectral domain. The compression can be achieved by retaining non-trivial values while zeroing out small entries. A threshold ( $\beta$ ) can then be applied to configure the compression rate where larger  $\beta$  values result in more zeros in the spectral domain feature maps.

As with existing CNNs [21, 16, 13, 36] which operate in the spatial domain, the elemental SpecNet, operating in

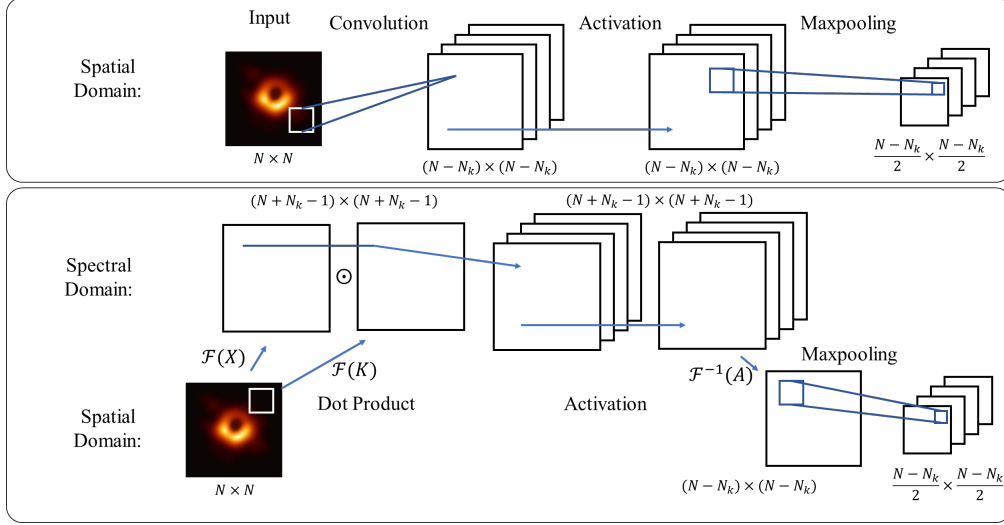


Figure 1. The standard convolutional block in the spatial and spectral domains. The top figure shows the standard convolutional block containing an input layer and one convolutional layer followed by an activation layer and a maxpooling layer. The bottom figure shows the convolutional block in SpecNet. The kernels are stored in the spatial domain while the feature maps are efficiently stored in the spectral domain. It is worth noting that the convolutional block of SpecNet can contain more than one convolutional layers between input and maxpooling layer.

the spectral domain, also consists of three layers: convolutional layers, activation layers, and pooling layers as shown at the bottom half of Fig. 1. In contrast to previous studies [32, 28, 9] that simply use the FFT to accelerate network training, SpecNet represents a new design of the network architecture for convolution, tensor compression, and activation in the spectral domain and can be applied to both forward and backward propagation in network training and inference.

### 3.1. Convolution in the Spectral Domain

Consider 2D-convolution with a stride of 1. In a standard convolutional layer, the output is computed by

$$y(i, j) = x * k = \sum_{m=0}^{M-1} \sum_{n=0}^{N-1} x(m, n) \cdot k(i - m, j - n), \quad (1)$$

where  $x$  is an input matrix of size  $(M, N)$ ;  $k$  is the kernel with dimension  $(N_k, N_k)$ , and  $*$  indicates 2D convolution. The output  $y$  in the spatial domain has dimensions  $(M', N')$ , where  $M' = M + N_k - 1$  and  $N' = N + N_k - 1$ . This process involves  $\mathcal{O}(M'N'N_k^2)$  multiplications.

Convolution can be implemented more efficiently in the spectral domain as

$$Y = X \odot K, \quad (2)$$

where  $X$  is the transformed input in the spectral domain by FFT  $X = \mathcal{F}(x)$ , and  $K$  is the corresponding kernel in

the spectral domain,  $K = \mathcal{F}(k)$ .  $\odot$  represents element-by-element multiplication, which requires equal dimensions for  $X$  and  $K$ . Therefore,  $x$  and  $k$  are zero-padded to match their dimensions  $(M', N')$ . Since there are various hardware optimizations for the FFT [22, 15, 32], it requires  $\mathcal{O}(M'N' \log(M'N'))$  complex multiplications. The computational complexity of (2) is  $\mathcal{O}(M'N')$  and so the overall complexity in the spectral domain is  $\mathcal{O}(M'N' \log(M'N'))$ . Depending on the size of the inputs and kernels, SpecNet can have a computational advantage over spatial convolution in some cases [32, 28]. However, SpecNet is focused on reducing memory consumption for applications that are primarily limited by the available memory.

The compression of  $Y$  involves a configurable threshold  $\beta$ , which forces entries in  $Y$  with small absolute values (those less than  $\beta$ ) to zero. This allows the thresholded map ( $\hat{Y}$ ) to be sparse and hence to store only the non-zero entries in  $\hat{Y}$ , thus saving memory.

The backward propagation step requires the calculation of the error  $\delta_X$  for the previous layers, and the gradients  $\Delta_K$  for  $k$ . Let  $\delta_Y$  be the error from the next layer, and  $X_0, k_0$  be the input and kernel of the convolutional layer stored in the forward propagation, respectively. Then

$$\begin{aligned} \delta_X &= \nabla_X L|_{X=X_0} = \delta_Y \odot K_0 \\ \Delta_K &= \nabla_K L|_{K=\mathcal{F}(k_0)} = \delta_Y \odot X_0, \end{aligned} \quad (3)$$

where  $L$  is the loss function. After obtaining its gradient in the spectral domain  $\Delta_K$ , the IFFT is applied. Then the

$N_k \times N_k$  matrix for the update of  $k$  can be expressed as

$$k_1 = k_0 + \lambda[\mathcal{F}^{-1}(\Delta_K)]_{N_k \times N_k}, \quad (4)$$

where  $\lambda$  is the learning rate. The kernels are updated after obtaining  $\Delta_K$ , the gradient in the spectral domain, by using the inverse FFT and downsampling.

Note that after the gradient update of  $\Delta_K$ , the kernel is further converted from the spectral domain back into the spatial domain using the inverse FFT to save kernel storage.

A more general case of 2D-convolution with arbitrary integer stride can be viewed as a combination of 2D-convolution with stride of 1 and uniform down-sampling, which can also be implemented in the spectral domain [32].

### 3.2. Activation Function in the Spectral Domain

In SpecNet, the activation function for the feature maps is designed to perform directly in the spectral domain. For each complex entry in the spectral feature map,

$$f(a + ib) = h(a) + ig(b) \quad (5)$$

where

$$h(x) = g(x) = \tanh(x) = \frac{e^x - e^{-x}}{e^x + e^{-x}}. \quad (6)$$

The tanh function is used in (5) as a proof-of-concept design for this study. Other activation functions may also be used, but must fulfill the following:

1. They allow inexpensive gradient calculation.
2. Both  $g(x)$  and  $h(x)$  are monotonic nondecreasing
3. The functions are odd, i.e.  $g(-x) = -g(x)$ .

The first and second rules are standard requirements for nearly all popular activation functions used in modern CNN design. The third rule in SpecNet is applied to preserve the conjugate symmetry structure of the spectral feature maps so that they can be converted back into real spatial features without generating pseudo phases. The 2D FFT is

$$X(p, q) = \mathcal{F}(x) = \sum_{m=0}^{M+N_k-2} \sum_{n=0}^{N+N_k-2} w_M^{pm} w_N^{qn} x(m, n)$$

where  $w_M = e^{-2\pi i/(M+N_k-1)}$ ,  $w_N = e^{-2\pi i/(N+N_k-1)}$ . If  $x$  is real, i.e., the conjugate of  $x$  is itself ( $\bar{x} = x$ ), then

$$\begin{aligned} & X(M + N_k - 1 - p_0, N + N_k - 1 - q_0) \\ &= \sum_{m=0}^{M+N_k-2} \sum_{n=0}^{N+N_k-2} w_M^{(M+N_k-1-p_0)m} w_N^{(N+N_k-1-q_0)n} x(m, n) \\ &= \sum_{m=0}^{M+N_k-2} \sum_{n=0}^{N+N_k-2} w_M^{-p_0 m} w_N^{-q_0 n} x(m, n) \quad (7) \\ &= \overline{X(p_0, q_0)} \end{aligned}$$

---

**Algorithm 1** Forward propagation of the convolutional block in spectral domain

---

**Input:** feature maps  $x$  from the last layer with size of  $M \times N$ ; kernel  $k$  ( $N_k \times N_k$ ); threshold  $\beta$ .

- 1: **if**  $x$  in the spectral domain **then**
- 2:     Set  $M' = M$ ,  $N' = N$  and  $X = x$ .
- 3: **else**
- 4:     Set  $M' = M + N_k - 1$  and  $N' = N + N_k - 1$ .
- 5: **end if**
- 6: **for**  $i = 1$  to  $M'$  **do**
- 7:     **for**  $j = 1$  to  $N'$  **do**
- 8:         **if**  $X$  is None **then**
- 9:              $\hat{x}(i, j) = x(i, j)$  if  $i \leq M$  and  $j \leq N$ , and  $\hat{x}(i, j) = 0$  otherwise.
- 10:         **end if**
- 11:          $\hat{k}(i, j) = k(i, j)$  if  $i \leq N_k$  and  $j \leq N_k$ , and  $\hat{k}(i, j) = 0$  otherwise.
- 12:         Calculate  $K = \mathcal{F}(\hat{k})$  and  $X = \mathcal{F}(\hat{x})$  if  $X$  is None.
- 13:     **end for**
- 14: **end for**
- 15:     Calculate  $Y$  after convolution according to (2).
- 16:     Obtain  $\hat{Y}$  where  $\hat{Y}(i, j) = Y(i, j)$  if  $|Y(i, j)| > \beta$ , and  $\hat{Y}(i, j) = 0$  otherwise.
- 17:     Get  $Z = f(\hat{Y})$  where  $f$  is defined in (5)

**Output:** The feature map in the spectral domain:  $Z$ .

---

Therefore,  $g(x)$  must be odd to retain the symmetry structure of the activation layer to ensure that

$$\begin{aligned} f(\overline{a + ib}) &= h(a) + ig(-b) \\ &= h(a) - ig(b) = \overline{h(a) + ig(b)}. \end{aligned} \quad (8)$$

If the symmetry structure of  $\delta_Y$  in (3) is also maintained, the gradients in the spatial domain will be real-valued after the inverse FFT in (4), and can be added to  $k_0$  directly.

Let  $X_0$  be the input to the activation layer in forward propagation, and  $\delta_Y$  be the error from the next layer. The error for the previous layer in backward propagation can be calculated by

$$\begin{aligned} \delta_X &= \{1 - [\tanh(\Re(X_0))]^2\} \odot \Re(\delta_Y) + \\ & \quad i\{1 - [\tanh(\Im(X_0))]^2\} \odot \Im(\delta_Y). \end{aligned} \quad (9)$$

### 3.3. Pooling Layers

The pooling methods in SpecNet are implemented in the spatial domain after transforming the activated frequency feature maps back into the spatial domain using the IFFT. As a result of the convolution and activation function design (which preserve conjugate symmetry in the spectral domain feature maps), the corresponding spatial feature maps are

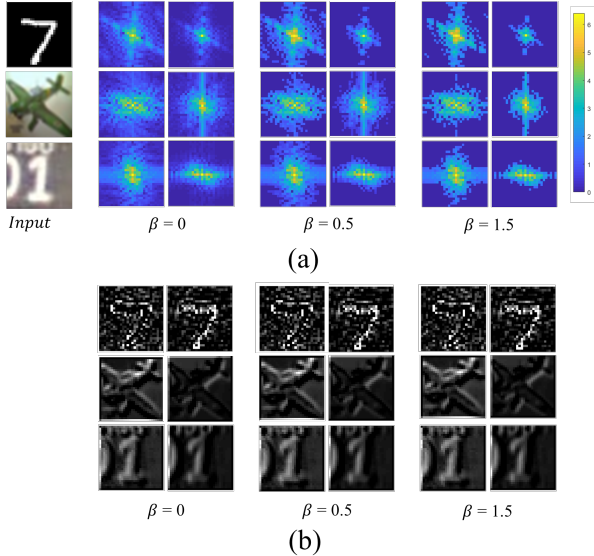


Figure 2. Feature maps of SpecDenseNet after the first convolutional layer for different inputs. (a) Feature maps after two different kernels in the spectral domain with three different thresholds  $\beta$ . (b) Feature maps, converted from the spectral domain to the spatial domain by utilizing the inverse Fourier transform with different thresholds  $\beta$ .

real valued and the same pooling operation (max pooling or average pooling) used in standard CNNs can be used seamlessly in SpecNet. The calculation of the error in backward propagation can be found in the standard approach [23]. Note that the error is in the spatial domain; if the previous layer is either an activation or convolutional layer, the error should be transformed into the spectral domain to get  $\delta_Y$  in (3) or (9).

### 3.4. Implementation Details

SpecNet stores the kernels in the spatial domain as  $N_k \times N_k$  matrices. Therefore, given the input feature maps in the spectral domain, each kernel should be upsampled to the size of the inputs by padding with zeros, and then transformed to the spectral domain with the FFT. The complete forward propagation of the convolutional block (including convolution and activation operations) in the spectral domain is shown in Algorithm 1.

## 4. Experiments

We demonstrate the feasibility of SpecNet using several benchmark datasets and by comparing the performance of SpecNet implementations of several state-of-the-art networks (LeNet, AlexNet, VGG16 and DenseNet) with their standard implementations.

### 4.1. Datasets

**MNIST** is a dataset of handwritten digits with 28 by 28 pixels each image, which is widely used for training and testing image processing, machine learning, and deep learning algorithms [20, 7]. In our experiment, 60,000 images were used for training and 10000 images were used for testing. The images were preprocessed by normalizing all pixel values to [0,1].

**CIFAR-10** is a ten class dataset of small colored natural images [17]. In our experiment, 50,000 images were used for training and 10,000 images were used for testing. All images of CIFAR 10 were resized to 32 by 32 pixels, and each channel was normalized with respect to its mean and standard deviation [13]. Standard data augmentation techniques [12] were also applied to the training set.

**SVHN** is a dataset consisting of colored digit images with 32 by 32 pixels each image [30]. The dataset contains 99289 images: 73257 images for training and 26032 images for testing. It is reported that state-of-art CNNs can achieve good performance on the dataset without data augmentation [13], therefore we do not use data augmentation for training. Images were channel-normalized in mean and standard deviation.

### 4.2. Training

Training and evaluation of all networks were performed on a desktop computer running a 64-bit Linux operating system (Ubuntu 16.04) with an Intel Core i7-7700K CPU and 32 GB DDR4 RAM and two Nvidia GeForce GTX 1080 graphic cards (Nvidia driver 384.130) with 2560 CUDA cores and 8GB GDDR5 RAM. All networks and algorithms (including comparisons) were implemented in MATLAB 2018a and Tensorflow 1.09.

All the networks were trained by mini batch stochastic gradient descent (SGD) with a batch size of 64 on MNIST, CIFAR, and SVHN. The initial learning rate was set to 0.1 and was reduced by half every 50 epochs. The momentum of the optimizer was set to 0.95 and a total of 300 epochs was trained to ensure convergence.

### 4.3. Results

First, we empirically show the impact when two different thresholds ( $\beta = 0.5$  and  $\beta = 1.5$ ) are applied to the feature maps. The results are shown in Fig. 2. Observe that the feature maps in the spectral domain are compressed (and sparsified), but that this does not significantly impact the feature maps in the spatial domain.

Next, we evaluated the proposed SpecNet using four widely used CNN architectures including LeNet-5 [21], AlexNet [18], VGG [19] and DenseNet [13]. We use the prefix ‘Spec’ to stand for the SpecNet implementation of each network. To ensure fair comparisons, the SpecNet networks used identical network hyper-parameters as the na-

Table 1. Detailed network structure for DenseNet and SpecDenseNet

DenseNet		
Layers	Output size	Structure
Input	32×32	Input
Convolution	32×32	3×3 kernel, BN, ReLU
Pooling	16×16	MaxPool (window size 2×2)
Dense Block	16×16	1×1 kernel, BN, ReLU 3×3 kernel, BN, ReLU ×6
Classification Layer	1×1	GlobalAveragePool Fully-connected, SoftMax (10 classes)
SpecDenseNet		
Layers	Output size	Structure
Input	32×32	Input
Convolutional Block	35×35	FFT
	35×35	FConv2D (3×3 kernels), Activation
	32×32	IFFT
Pooling	16×16	MaxPool (window size 2×2)
	19×19	FFT
Dense Block	19×19	FConv2D (64 1×1 kernels), Activation
	19×19	FConv2D (64 3×3 kernels), Activation ×6
	16×16	IFFT
Classification Layer	1×1	GlobalAveragePool Fully-connected, SoftMax (10 classes)

tive spatial domain implementations. The experiments also use the same conditions for image preprocessing, parameter initialization, and optimization settings. For example, architectures for DenseNet and SpecDenseNet are in Table 1. The other three networks are detailed in the supplementary material. The experimental results on MNIST, CIFAR-10 and SVHN are shown in Fig. 3.

Figures 3(a)(b)(c) compare the memory usage of the SpecNet implementations of four different networks over a range of beta values from 0.5 to 1.5. We compute relative memory consumption and error by: memory (error) of SpecNet / the memory (error) in the original implementations. When compared with their original models, all SpecNet implementations of the four networks can save at least 50% memory with negligible loss of accuracy, indicating the feasibility of compressing feature maps within SpecNet framework. With increasing  $\beta$  value, all models show monotonic reduction in memory usage. The rates of memory reduction are different between different network architectures, which is likely caused by different feature representations in the various network designs.

Figures 3(d)(e)(f) compare the relative error of the SpecNet implementation for the four different networks over the same range of  $\beta$  values from 0.5 to 1.5. While the SpecNet typically compresses the models, there is penalty in the form of increased error in comparison to the original model with full spatial feature maps. The average accuracy of SpecAlexNet, SpecVGG, and SpecDenseNet can be higher than 95% when  $\beta$  is smaller than 1.0.

Figures 4(a)(b)(c) show the relative memory use ( $\beta = 0.7$ ) during the training process. We recorded average memory consumption of each epoch and compare it with memory in the original implementations. The memory consumption gradually improves with the training epochs, and the

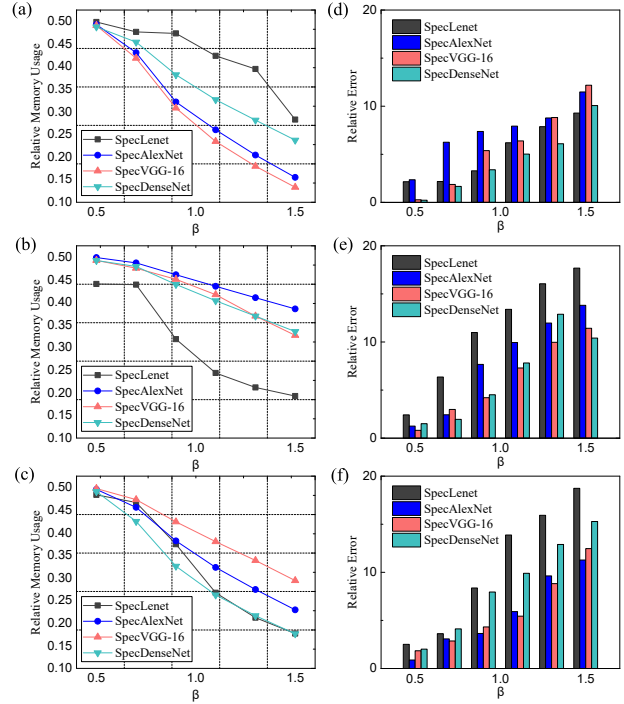


Figure 3. Memory consumption and testing performance of SpecNet compared with LeNet, AlexNet, VGG, and DenseNet [21, 18, 19, 13, 37] on three datasets. To make the comparison fair, we retain the analogous structures which we call SpecLeNet, SpecAlexNet, SpecVGG and SpecDenseNet. (a)(b)(c) relative memory consumption and (d)(e)(f) relative error of SpecNets tested on MNIST, CIFAR-10 and SVHN.

peak value tends to occur when the model has converged.

Table 2 shows a comparison between SpecNet and other recently published memory-efficient algorithms. The experiments investigate memory usage when training VGG and DenseNet on the CIFAR-10 dataset. For each algorithm, we selected most memory efficient performance that still retains testing accuracy of at least 90%. The SpecNet outperformed all the listed algorithms and resulted in the lowest memory usage while maintaining high testing accuracy. It is notable that SpecNet is independent of the work listed in the table, and these techniques can be applied along with SpecNet to further reduce memory consumption.

Fig. 5 shows the training curve of the SpecNet implementations of four different networks with their implementations in spatial domain. In order to make fair comparison, we maintain the same training hyper parameters, such as batch size, learning rate and kernel weights initialization. From the training curve, the SpecNet implementations shows very close convergence speed as the implementations in spatial domain. Section 3 also showed that the computation speed is related to the size of the inputs and kernels, and SpecNet is advantageous in some cases. Therefore, training speed of SpecNet is very comparable with the network in

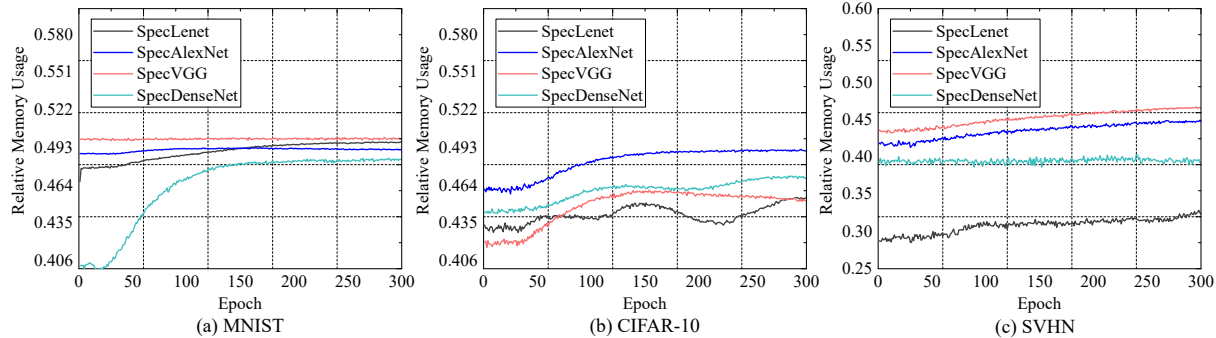


Figure 4. Memory consumption of SpecNet ( $\beta = 0.7$ ) during training compared with the original implementation of LeNet, AlexNet, VGG, and DenseNet on MNIST, CIFAR-10 and SVHN.

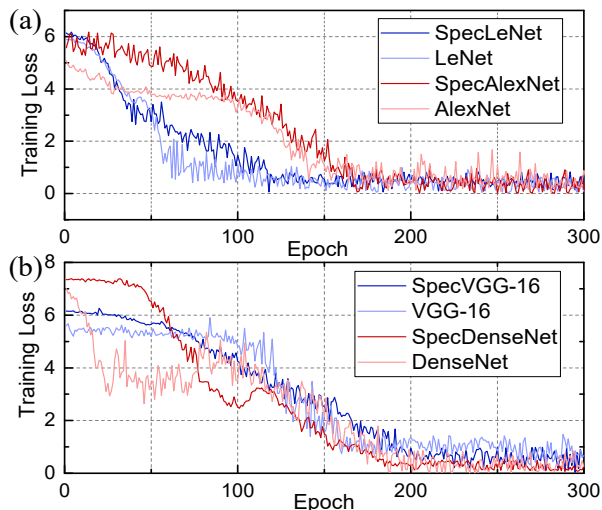


Figure 5. Training curves of SpecNet comparing with LeNet, AlexNet, VGG-16 on CIFAR-10 dataset.

spatial domain, but with the added benefit of memory efficiency.

The relative memory consumption and error can be computed by: memory (error) of SpecNet / the memory (error) in the original implementations. When compared with the original models, all SpecNet implementations of the four networks can save at least 50% memory with negligible loss of accuracy, indicating the feasibility of compressing feature maps within SpecNet framework. With increasing  $\beta$  value, all models show monotonic reduction in memory usage. The rates of memory reduction are different between different network architectures, which is likely caused by different feature representations in the various network designs.

## 5. Conclusion

We have introduced a new Convolutional Neural Network architecture called SpecNet, which performs both the convolution and the activation operations in the spectral do-

Table 2. Comparison of relative memory usage for different memory efficient implementations applied to VGG and DenseNet. All the methods are tested on CIFAR-10.

	VGG	DenseNet
INPLACE-ABN [35]	0.52	0.58
Chen Meng et al. [29]	0.65	0.55
Memory-Efficient DenseNets [31]	N/A	0.44
vDNN [33]	0.38	0.39
<b>SpecNet</b>	<b>0.37</b>	<b>0.37</b>

main. By setting a configurable threshold to force small values in the feature maps in the spectral domain to zero, the feature maps of SpecNet can be stored sparsely. SpecNet also employs a special activation function that preserves the sparsity of the feature maps and helps ensure training convergence. We have evaluated SpecNet on three competitive object recognition benchmark tasks (MNIST, CIFAR-10, and SVHN), and demonstrated the performance of SpecNet implementation of state-of-the-art (LeNet, AlexNet, VGG16 and DenseNet) to show the efficacy and efficiency of memory reduction. In some cases, SpecNet can reduce memory consumption by about 60% without significant loss of performance.

Our experimental hyper-parameter settings were identical to those of CNN in the spatial domain. Further memory reduction and performance improvement for SpecNet can be achieved by using more reasonable data scaling, dedicated network architecture and optimization settings tailored for SpecNet. Transform methods other than the FFT such as DCT, Wavelet transform, can also be incorporated into SpecNet to promote energy concentration for memory reduction.

It is also notable that SpecNet is only focused on the sparse storage of feature maps in the spectral domain. In the future, we plan to merge other methods, such as model compression and scheduling, with SpecNet to further improve memory usage.

## References

- [1] R. Andri, L. Cavigelli, D. Rossi, and L. Benini. Yodan: An architecture for ultralow power binary-weight cnn acceleration. *IEEE Transactions on Computer-Aided Design of Integrated Circuits and Systems*, 37(1):48–60, Jan 2018. 2
- [2] Sayed Omid Ayat, Mohamed Khalil-Hani, Ab Hadi Ab Rahman, and Hamdan Abdellatef. Spectral-based convolutional neural network without multiple spatial-frequency domain switchings. *Neurocomputing*, 364:152–167, 2019. 1
- [3] Soravit Changpinyo, Mark Sandler, and Andrey Zhmoginov. The power of sparsity in convolutional neural networks. *CoRR*, abs/1702.06257, 2017. 2
- [4] Tianqi Chen, Bing Xu, Chiyuan Zhang, and Carlos Guestrin. Training deep nets with sublinear memory cost. *CoRR*, abs/1604.06174, 2016. 1, 2
- [5] Yu Cheng, Duo Wang, Pan Zhou, and Tao Zhang. A survey of model compression and acceleration for deep neural networks. *CoRR*, abs/1710.09282, 2017. 1
- [6] Matthieu Courbariaux and Yoshua Bengio. Binarynet: Training deep neural networks with weights and activations constrained to +1 or -1. *CoRR*, abs/1602.02830, 2016. 1, 2
- [7] Li Deng. The mnist database of handwritten digit images for machine learning research [best of the web]. *IEEE Signal Processing Magazine*, 29(6):141–142, 2012. 5
- [8] Emily L Denton, Wojciech Zaremba, Joan Bruna, Yann LeCun, and Rob Fergus. Exploiting linear structure within convolutional networks for efficient evaluation. In Z. Ghahramani, M. Welling, C. Cortes, N. D. Lawrence, and K. Q. Weinberger, editors, *Advances in Neural Information Processing Systems 27*, pages 1269–1277. Curran Associates, Inc., 2014. 1, 2
- [9] Shin Fujieda, Kohei Takayama, and Toshiya Hachisuka. Wavelet convolutional neural networks for texture classification. *CoRR*, abs/1707.07394, 2017. 2, 3
- [10] Suyog Gupta, Ankur Agrawal, Kailash Gopalakrishnan, and Pritish Narayanan. Deep learning with limited numerical precision. In *International Conference on Machine Learning*, pages 1737–1746, 2015. 2
- [11] Stephen Jose Hanson and Lorien Y. Pratt. Comparing biases for minimal network construction with back-propagation. In D. S. Touretzky, editor, *Advances in Neural Information Processing Systems 1*, pages 177–185. Morgan-Kaufmann, 1989. 1, 2
- [12] Kaiming He, Xiangyu Zhang, Shaoqing Ren, and Jian Sun. Deep residual learning for image recognition. In *The IEEE Conference on Computer Vision and Pattern Recognition (CVPR)*, June 2016. 1, 5
- [13] Gao Huang, Zhuang Liu, Laurens van der Maaten, and Kilian Q. Weinberger. Densely connected convolutional networks. In *The IEEE Conference on Computer Vision and Pattern Recognition (CVPR)*, July 2017. 1, 2, 5, 6
- [14] Animesh Jain, Amar Phanishayee, Jason Mars, Lingjia Tang, and Gennady Pekhimenko. Gist: Efficient data encoding for deep neural network training. In *45th ACM/IEEE Annual International Symposium on Computer Architecture, ISCA 2018, Los Angeles, CA, USA, June 1-6, 2018*, pages 776–789, 2018. 1, 2
- [15] Armin Kappeler, Sushobhan Ghosh, Jason Holloway, Oliver Cossairt, and Aggelos Katsaggelos. Ptychnet: Cnn based fourier ptychography. In *2017 IEEE International Conference on Image Processing (ICIP)*, pages 1712–1716. IEEE, 2017. 3
- [16] Alex Krizhevsky. One weird trick for parallelizing convolutional neural networks. *arXiv preprint arXiv:1404.5997*, 2014. 2
- [17] Alex Krizhevsky and Geoffrey Hinton. Learning multiple layers of features from tiny images. Technical report, Citeseer, 2009. 5
- [18] Alex Krizhevsky, Ilya Sutskever, and Geoffrey E Hinton. Imagenet classification with deep convolutional neural networks. In F. Pereira, C. J. C. Burges, L. Bottou, and K. Q. Weinberger, editors, *Advances in Neural Information Processing Systems 25*, pages 1097–1105. Curran Associates, Inc., 2012. 5, 6
- [19] Alex Krizhevsky, Ilya Sutskever, and Geoffrey E Hinton. Imagenet classification with deep convolutional neural networks. In F. Pereira, C. J. C. Burges, L. Bottou, and K. Q. Weinberger, editors, *Advances in Neural Information Processing Systems 25*, pages 1097–1105. Curran Associates, Inc., 2012. 5, 6
- [20] Yann LeCun, Yoshua Bengio, and Geoffrey Hinton. Deep learning. *nature*, 521(7553):436, 2015. 1, 5
- [21] Yann LeCun, LD Jackel, Leon Bottou, A Brunot, Corinna Cortes, JS Denker, Harris Drucker, I Guyon, UA Muller, Eduard Sackinger, et al. Comparison of learning algorithms for handwritten digit recognition. In *International conference on artificial neural networks*, volume 60, pages 53–60. Perth, Australia, 1995. 2, 5, 6
- [22] Jae-Han Lee, Minhyeok Heo, Kyung-Rae Kim, and Chang-Su Kim. Single-image depth estimation based on fourier domain analysis. In *The IEEE Conference*

- on *Computer Vision and Pattern Recognition (CVPR)*, June 2018. 3
- [23] James Leonard and MA Kramer. Improvement of the backpropagation algorithm for training neural networks. *Computers & Chemical Engineering*, 14(3):337–341, 1990. 5
- [24] Hao Li, Asim Kadav, Igor Durdanovic, Hanan Samet, and Hans Peter Graf. Pruning filters for efficient convnets. *CoRR*, abs/1608.08710, 2016. 2
- [25] Yuchao Li, Shaohui Lin, Baochang Zhang, Jianzhuang Liu, David Doermann, Yongjian Wu, Feiyue Huang, and Rongrong Ji. Exploiting kernel sparsity and entropy for interpretable cnn compression. In *The IEEE Conference on Computer Vision and Pattern Recognition (CVPR)*, June 2019. 1
- [26] Baoyuan Liu, Min Wang, Hassan Foroosh, Marshall Tappen, and Marianna Pensky. Sparse convolutional neural networks. In *The IEEE Conference on Computer Vision and Pattern Recognition (CVPR)*, June 2015. 2
- [27] Fang Liu, Bochen Guan, Zhaoye Zhou, Alexey Samsonov, Humberto Rosas, Kevin Lian, Ruchi Sharma, Andrew Kanarek, John Kim, Ali Guermazi, et al. Fully automated diagnosis of anterior cruciate ligament tears on knee mr images by using deep learning. *Radiology: Artificial Intelligence*, 1(3):180091, 2019. 1
- [28] Michael Mathieu, Mikael Henaff, and Yann LeCun. Fast training of convolutional networks through ffts. *arXiv preprint arXiv:1312.5851*, 2013. 2, 3
- [29] Chen Meng, Minmin Sun, Jun Yang, Minghui Qiu, and Yang Gu. Training deeper models by gpu memory optimization on tensorflow. In *Proc. of ML Systems Workshop in NIPS*, 2017. 7
- [30] Yuval Netzer, Tao Wang, Adam Coates, Alessandro Bissacco, Bo Wu, and Andrew Y. Ng. Reading digits in natural images with unsupervised feature learning. In *NIPS Workshop on Deep Learning and Unsupervised Feature Learning 2011*, 2011. 5
- [31] Geoff Pleiss, Danlu Chen, Gao Huang, Tongcheng Li, Laurens van der Maaten, and Kilian Q Weinberger. Memory-efficient implementation of densenets. *arXiv preprint arXiv:1707.06990*, 2017. 1, 2, 7
- [32] Harry Pratt, Bryan M. Williams, Frans Coenen, and Yalin Zheng. Fcnn: Fourier convolutional neural networks. In *ECML/PKDD*, 2017. 2, 3, 4
- [33] Minsoo Rhu, Natalia Gimelshein, Jason Clemons, Arslan Zulfiqar, and Stephen W Keckler. vdn: Virtualized deep neural networks for scalable, memory-efficient neural network design. In *The 49th Annual IEEE/ACM International Symposium on Microarchitecture*, page 18. IEEE Press, 2016. 7
- [34] Oren Rippel, Jasper Snoek, and Ryan P. Adams. Spectral representations for convolutional neural networks. In *Proceedings of the 28th International Conference on Neural Information Processing Systems - Volume 2*, NIPS’15, pages 2449–2457, Cambridge, MA, USA, 2015. MIT Press. 1, 2
- [35] Samuel Rota Bul, Lorenzo Porzi, and Peter Kotschieder. In-place activated batchnorm for memory-optimized training of dnns. In *The IEEE Conference on Computer Vision and Pattern Recognition (CVPR)*, June 2018. 7
- [36] Christian Szegedy, Sergey Ioffe, Vincent Vanhoucke, and Alexander A Alemi. Inception-v4, inception-resnet and the impact of residual connections on learning. In *Thirty-First AAAI Conference on Artificial Intelligence*, 2017. 2
- [37] Yan Wang, Lingxi Xie, Chenxi Liu, Siyuan Qiao, Ya Zhang, Wenjun Zhang, Qi Tian, and Alan Yuille. Sort: Second-order response transform for visual recognition. In *The IEEE International Conference on Computer Vision (ICCV)*, Oct 2017. 6
- [38] Yunhe Wang, Chang Xu, Chao Xu, and Dacheng Tao. Beyond filters: Compact feature map for portable deep model. In *ICML*, volume 70 of *Proceedings of Machine Learning Research*, pages 3703–3711. PMLR, 2017. 1, 2
- [39] Wei Wen, Chunpeng Wu, Yandan Wang, Yiran Chen, and Hai Li. Learning structured sparsity in deep neural networks. In D. D. Lee, M. Sugiyama, U. V. Luxburg, I. Guyon, and R. Garnett, editors, *Advances in Neural Information Processing Systems 29*, pages 2074–2082. Curran Associates, Inc., 2016. 2
- [40] Jiaxiang Wu, Cong Leng, Yuhang Wang, Qinghao Hu, and Jian Cheng. Quantized convolutional neural networks for mobile devices. In *The IEEE Conference on Computer Vision and Pattern Recognition (CVPR)*, June 2016. 1, 2
- [41] Junzhe Zhang, Sai Ho Yeung, Yao Shu, Bingsheng He, and Wei Wang. Efficient memory management for gpu-based deep learning systems. *arXiv preprint arXiv:1903.06631*, 2019. 1, 2
- [42] Xiangyu Zhang, Jianhua Zou, Xiang Ming, Kaiming He, and Jian Sun. Efficient and accurate approximations of nonlinear convolutional networks. In *The IEEE Conference on Computer Vision and Pattern Recognition (CVPR)*, June 2015. 2